Inorg. Chem. **2006**, *45*, 8563–8574

Investigation of the Pronounced Medium Effects Observed in the Voltammetry of the Highly Charged Lacunary Anions $[\alpha\text{-}SiW_{11}O_{39}]^{8-}$ and $[\alpha\text{-}PW_{11}O_{39}]^{7-}$

Si-Xuan Guo,[†] Andrew W. A. Mariotti,[‡] Christine Schlipf,[‡,§] Alan M. Bond,*[,†] and Anthony G. Wedd*[,‡]

School of Chemistry, Monash University, Clayton, 3800, Victoria, Australia, and School of Chemistry, The University of Melbourne, Parkville, Victoria, 3010, Australia and the Bio21 Molecular Science and Biotechnology Institute, 30 Flemington Road, Parkville, Victoria, 3010, Australia

Received June 15, 2006

A detailed study is reported of the influence of protons, metal cations, and media on the redox chemistry of lacunary anions $[\alpha\text{-}SiW_{11}O_{39}]^{8-}$ and $[\alpha\text{-}PW_{11}O_{39}]^{7-}$ of high formal negative charge. Each anion displayed a single chemically reversible one-electron reduction process in carefully dried aprotic CH_3CN solution. This process was detected at very negative potentials just prior to the solvent limit. Addition of 0.3 equiv of acid gave rise to a new reduction process at considerably less negative potentials, which is attributed to formation of the protonated species $[SiW_{11}O_{38}(OH)]^{7-}$ and $[PW_{11}O_{38}(OH)]^{6-}$. Voltammograms derived from simulations based on a double-square scheme are in excellent agreement with experiment. Previous data reported the presence of several processes in CH_3CN and appear to have been influenced by the presence of protons and/or adventitious water. Not surprisingly, protonation reactions coupled to charge transfer contribute significantly to the voltammetry of these lacunary anions in buffered aqueous media over the pH range 2–6. A multi-square-scheme mechanism allowed the essential thermodynamic and kinetic features of this system to be captured and an assessment of the relative significance of possible individual pathways. The high formal anionic charges of $[SiW_{11}O_{39}]^{8-}$ and $[PW_{11}O_{39}]^{7-}$ appear to provide highly basic reduced forms that are able to abstract protons from water to produce protonated species which are reduced at potentials more than a volt less negative than those for the processes $[SiW_{11}O_{39}]^{8-/9-}$ and $[PW_{11}O_{39}]^{7-/8-}$ found in dry aprotic media.

Introduction

The influence of the solvent medium, supporting electrolyte, and added cation and proton concentration on the redox chemistry of polyoxometalate anions has important consequences for their electron-transfer and catalytic properties.[1−5] Voltammetric methods represent a very useful method of understanding the effects of the chemical environment on the redox chemistry of these cluster anions. However, the electrochemistry is often complex and detailed simulations are needed to understand the role of the medium. Recently, simulations of the voltammetry of both Keggin and Dawson anion systems (such as $[\alpha\text{-}H_2W_{12}O_{40}]^{6-}$, $[\alpha\text{-}S_2Mo_{18}O_{62}]^{4-}$, $[\gamma^*\text{-}S_2W_{18}O_{62}]^{4-}$, and $[\alpha\text{-}P_2W_{18}O_{62}]^{6-}$) have been used for quantitative interpretation of electron-transfer steps coupled with acid−base equilibria.[3,6−8] In addition, recent studies of the voltammetry of $[\alpha\text{-}SiW_{12}O_{40}]^{4-}$ and $[\alpha\text{-}PW_{12}O_{40}]^{3-}$ in

* To whom correspondence should be addressed. E-mail: alan.bond@sci.monash.edu.au (A.M.B.); agw@unimelb.edu.au (A.G.W.).
[†] Monash University.
[‡] The University of Melbourne and Bio21 Institute.
[§] Current address: Department of Chemistry, University of Bielefeld, Germany.

(1) Pope, M. T. *Heteropoly and Isopoly Oxometalates*; Springer-Verlag: Berlin, 1983.
(2) Sadakane, M.; Steckhan, E. *Chem. Rev.* **1998**, *98*, 219.
(3) Himeno, S.; Takamoto, M.; Santo, R.; Ichimura, *Bull. Chem. Soc. Jpn.* **2005**, *78*, 95.
(4) Hill, C. L. *Comprehensive Coordination Chemistry II*; McCleverty, J. A., Meyer, T. J., Eds.; Elsevier: Amsterdam, 2004; Vol. 4.
(5) Pope, M. T. *Comprehensive Coordination Chemistry II*; McCleverty, J. A., Meyer, T. J., Eds.; Elsevier: Amsterdam, 2004; Vol. 4.
(6) Bond, A. M.; Vu, T.; Wedd, A. G. *J. Electroanal. Chem.* **2000**, *494*, 96.
(7) Richardt, P. J. S.; Gable, R. W.; Bond, A. M.; Wedd, A. G. *Inorg. Chem.* **2001**, *40*, 703.
(8) Prenzler, P. D.; Boskovic, C.; Bond, A. M.; Wedd, A. G. *Anal. Chem.* **1999**, *71*, 3650.

10.1021/ic061081o CCC: $33.50
Published on Web 09/19/2006

our laboratories have provided a detailed understanding of the influence of pH and solvent.[9]

A major reason for the pronounced influence of the medium on polyoxometalate chemistry is the high formal negative charges on these species, which may lead to significant interactions with protons and other cations present in solution. For example, lacunary polyoxometalate anions are derived by formal removal of one or more $[M^{VI}O]^{4+}$ units from the classic precursors such as the Keggin anions with their $XM_{12}O_{40}$ frameworks (M = Mo, W; Structure I) and

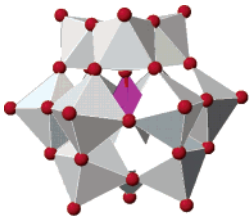

Structure I $[XM_{12}O_{40}]^{n-}$

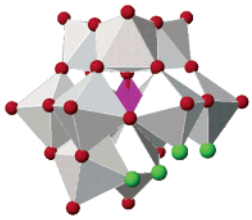

Structure II $[XM_{11}O_{39}]^{(n+4)-}$

hence may have exceptionally high anionic charges. They are of considerable interest as derivative synthons in the search for extended networks of polyoxo anions with targeted properties (see, for example, refs 10 and 11).

The voltammetry of the lacunary anion $[SiW_{11}O_{39}]^{8-}$ (Structure II) which has an formal anionic charge of 8−, features two processes in aqueous media (acetate buffer; pH 4.7; 0.5 M NaCl). Both are shifted to more positive potentials at pH 2, implying that the charge transfer processes are coupled extensively with acid−base chemistry in aqueous media.[12−16] Analogous pH-dependent behavior is observed for $[PW_{11}O_{39}]^{7-}$ in water.[13−16]

The available data suggest that salts of both lacunary systems feature the unprotonated $[SiW_{11}O_{39}]^{8-}$ and $[PW_{11}O_{39}]^{7-}$ anions in the solid state.[17] Elemental analysis is consistent with the formulations $K_6Na_2SiW_{11}O_{39}\cdot 13H_2O$ and $K_7PW_{11}O_{39}\cdot 12H_2O$, i.e., that there are eight and seven K^+/Na^+ cations present, respectively. Interestingly, the locations of only three of the eight K^+ cations and none of the water molecules are defined in the available crystal structure of α-$K_8SiW_{11}O_{39}\cdot 13H_2O$.[18]

In aqueous solution, $[SiW_{11}O_{39}]^{8-}$ is able to bind three protons (pK_a: 1.6, 4.0, 5.2; $TrisH^+$ buffer, 1.0 M; K^+, 0.08 M).[19,20] Although the role of other cations present in the buffer has not been established, it is probable that both lacuna are protonated and/or ion paired in solution rather than being present as anions of charges as high as 7− or 8−.

The salts $[Bu_4N]_4H_4[SiW_{11}O_{39}]$ and $[Bu_4N]_4H_3[PW_{11}O_{39}]$ have been isolated in substance.[21] When dissolved in CH_3CN (0.1 M Bu_4NClO_4), they are reported to exhibit three and two one-electron voltammetric processes, respectively. This behavior is significantly different from that observed in water. However, the roles of proton, electrolyte cations, and adventitious water, as will emerge from this study, have not been established in aprotic acetonitrile.

The present work reports a detailed examination of the influence of protons, other cations, and the nature of the electrolyte medium on the solution redox chemistry of the α forms of the anions $[SiW_{11}O_{39}]^{8-}$ and $[PW_{11}O_{39}]^{7-}$. $[Hept_4N]^+$ salts have been synthesized by phase transfer and their voltammetry studied in aprotic acetonitrile. Experiments were also undertaken in buffered aqueous media in the pH range 2.0−6.8 and as a function of ionic strengths at pH 4.6. Simulations of the observed voltammetry were used to explore the essential nature of the reduction mechanism in both buffered aqueous and aprotic acetonitrile media. While the extensive solution equilibria of both these lacunary anions introduce too many unknown parameters (equilibrium and rate constants) to allow a fully quantitative interpretation of all aspects of the observed voltammetry, the essential features are established. These provide an explanation for the very large differences in reversible potentials encountered in the different environments.

Experimental Section

Reagents. $K_4[\alpha\text{-}SiW_{12}O_{40}]$, $K_8[\alpha\text{-}SiW_{11}O_{39}]\cdot 13H_2O$, and $K_7[\alpha\text{-}PW_{11}O_{39}]\cdot 12H_2O$ were synthesized according to literature procedures.[22,23] The synthesis of a $[Hept_4N]^+$ salt of $[SiW_{11}O_{39}]^{8-}$ involved use of a phase-transfer process adapted from a published protocol.[24] A solution of $Hept_4NBr$ (78.5 mg, 16.0 mmol) in toluene (10 mL) was added dropwise with vigorous stirring to a solution of $K_8SiW_{11}O_{39}\cdot 13H_2O$ (64.4 mg, 2.00 mmol) in water (10 mL). The mixture was stirred for a further 30 min before allowing the layers to separate in a separatory funnel. The upper toluene-rich layer was collected in a Schlenk flask and the excess solvent removed, leaving a white solid (113 mg, 95%), formulated as $[Hept_4N]_8[\alpha\text{-}SiW_{11}O_{39}]$.[25] IR (KBr disk): 2957, 2925, 2851, 1627, 1567, 1378, 996, 908, 799, 722, 539 cm^{-1}. ^1H NMR (d_3-CH_3CN): 3.11 (m), 2.23 (m), 1.61 (m), 1.33 (m), 0.90 (m). ^{13}C NMR (d_3−CH_3CN) [δ (ppm)]: 14.4 (−CH_3), 22.5 (−CH_2−CH_3), 23.3 (−CH_2−C_2H_5), 26.9 (−CH_2−C_3H_7), 29.4 (−CH_2−C_4H_9), 32.3 (N−CH_2−CH_2−), 59.5 ppm (N−CH_2−). Anal. Found: C, 48.22; H, 8.65; Br, 5.11; N, 1.96. The higher C, H, and N ratios suggests the

(9) Guo, S. X.; Mariotti, A. W. A.; Schlipf, C.; Bond, A. M.; Wedd, A. G. *J. Electroanal. Chem.* **2006**, *591*, 7.
(10) Gouzerh, P.; Proust, A. *Chem. Rev.* **1998**, *98*, 77.
(11) Marcoux, P. R.; Hasenknopf, B.; Vaissermann, J.; Gouzerh, P., *Eur. J. Inorg. Chem.* **2003**, 13, 2406.
(12) Tézé, A.; Hervé, G. *J. Inorg. Nucl. Chem.* **1977**, *39*, 999.
(13) Couto, F. A. R. S.; Cavaleiro, A. M. V.; Pedrosa de Jesus, J. D.; Simão, J. E. J. *Inorg. Chim. Acta* **1998,** *281*, 225.
(14) Mueller, A.; Dloczik, L.; Diemann, E.; Pope, M. T. *Inorg. Chim. Acta* **1997,** *257*, 231.
(15) Toth, J. E.; Anson, F. C. *J. Electroanal. Chem.* **1988**, *256*, 361.
(16) Souchay, P.; Teze, A. *C. R. Seances Acad. Sci., Ser. C* **1969,** *268*, 804.
(17) Balula, M. S.; Gamelas, J. A.; Carapuca, H. M.; Cavaleiro, A. M. V.; Schlindwein, W. *Eur. J. Inorg. Chem.* **2004**, *3*, 619.
(18) Matsumoto, K. Y.; Sasaki, Y. *Bull. Chem. Soc. Jpn.* **1976**, *49*, 156.
(19) Contant, R.; Ciabrini, J. P. *J. Chem. Res. (S)* **1982**, *2*, 50.
(20) Pochon, P.; Moisy, P.; Donnet, L.; de Brauer, C.; Blanc, P. *Phys. Chem. Chem. Phys.* **2000,** *2*, 3813.
(21) Balula, M. S.; Gamelas, J. A.; Carapuca, H. M.; Cavaleiro, A. M. V.; Schlindwein, W. *Eur. J. Inorg. Chem.* **2004**, *3*, 619.
(22) Haraguchi, N.; Okaue, Y.; Isobe, T.; Matsuda, Y. *Inorg. Chem.* **1994**, *33*, 1015.
(23) Tézé, A.; Hervé, G. *Inorg. Synth.* **1990**, *27*, 85.
(24) Katsoulis, D. E.; Pope, M. T. *J. Chem. Soc., Dalton Trans.* **1989**, *8*, 1483.

(25) From the elemental analysis, the formula of the compound which best fits is $[Hept_4N]_8[SiW_{11}O_{39}]\cdot 3Hept_4NBr\cdot 2KCl$.

presence of $Hept_4NBr$ and also KBr (due to the high Br content) in the compound. For three $Hept_4NBr$ and two KBr molecules in the compound, $C_{308}H_{660}Br_5K_2N_{11}O_{39}SiW_{11}$ (i.e., $[Hept_4N]_8[SiW_{11}O_{39}]\cdot 3Hept_4NBr\cdot 2KBr$) requires: C, 48.23; H 8.67; Br 5.21; N 2.01.

The synthesis of the $[Hept_4N]^+$ salt of $[PW_{11}O_{39}]^{7-}$ followed an analogous procedure. To a solution of $K_7PW_{11}O_{39}\cdot 12H_2O$ (28.9 mg, 100 μmol) in water (5 mL) a solution of $[(n\text{-}C_7H_{15})N]Br$ (34.0 mg, 700 μmol) in toluene (5 mL) was added dropwise with vigorous stirring. The mixture was stirred for about 15 min and allowed to settle, and the organic layer was transferred to a round-bottom flask. The solvent was then removed on a rotary evaporator, and the colorless product formulated as $[Hept_4N]_7[\alpha\text{-}PW_{11}O_{39}]$[25] was dried at the pump for 1 h at 50 °C. ^{31}P NMR (d_3-MeCN, 161.8 MHz): −7.97 ppm. ^{13}C NMR (d_3-MeCN, 100.5 MHz): 14.4 ($-CH_3$), 22.5 ($-CH_2-CH_3$), 23.3 ($-CH_2-C_2H_5$), 26.9 ($-CH_2-C_3H_7$), 29.5 ($-CH_2-C_4H_9$), 32.3 ($N-CH_2-CH_2-$), 59.4 ppm ($N-CH_2-$). ^{1}H NMR (d_3-MeCN, 399.7 MHz): 0.90 (m), 1.31 (m), 1.35 (m), 1.62 (m), 3.13−3.17 ppm (m).

Bu_4NPF_6 (Aldrich; 98%) was recrystallized twice from ethanol.[26] In experiments undertaken in what is referred to as "dry" CH_3CN, a commercial solvent (Ajax Finechem; UV anhydrous, 99.9%) was purified according to a literature procedure:[27] K_2CO_3 (60 g) was dried overnight in a Schlenk flask under vacuum at 130 °C then allowed to cool. CH_3CN (1700 mL) was added to the flask, and N_2 was bubbled through the mixture for 30 min before stirring overnight under N_2 at room temperature. A distillation apparatus was assembled with P_2O_5 in the distillation flask and with K_2CO_3 in the receiver flask. The apparatus was pumped under vacuum overnight at room temperature, while the K_2CO_3 was dried at 130 °C. After being allowed to cool, the apparatus was subjected to four pump/N_2 fill cycles and the CH_3CN was transferred to the distillation flask via a cannula under N_2. The CH_3CN was then distilled off the P_2O_5 and was collected in the receiver flask containing the dry K_2CO_3. This distillate was redistilled over dry K_2CO_3 using the same technique and was collected in a solvent tower for storage under N_2 (boiling range 82−83 °C). All other chemical reagents were used as received from the manufacturer. Hydrochloric, acetic, chloroacetic, citric, and formic acids, as well as $KOOCCH_3$ and K_2HPO_4, were supplied by Ajax. Details of suppliers of other reagents are as follows. Ferrocene (Merck), 2-[*N*-morpholino]ethanesulfonic acid hydrate (MES; Sigma), $K_3[Fe(CN)_6]$ (Hopkin and Williams), KH_2PO_4 (BDH), KOH (Chemsupply), KCl (BDH), and NaCl (BDH).

The buffer solutions, also used as electrolytes in aqueous media, were prepared from the following solutions (pH was adjusted either with KOH or HCl): 0.1 M KCl + 0.1 M buffer (chloroacetate, pH 2.8; citrate, pH 3.1; formate, pH 3.8 and 4.2; acetate, pH 4.6; MES, pH 6.0 and phosphate, pH 6.8). Experiments at pH 2.1 were undertaken with 0.01 M HCl + 0.1 M KCl. While not a strictly buffered solution, the fact that the hydrogen ion concentration is an order of magnitude higher than that of the polyoxometalate anion (1 mM) means that the H^+ concentration also remains approximately constant in voltammetric studies in this medium.

Instrumentation and Procedures. Voltammetric data were obtained using either an Autolab (PGSTAT100) (Eco Chemie, Utrecht, Netherlands) or a Maclab (ADInstruments Mac/2e) computer-controlled electrochemical workstations. A standard three-electrode arrangement was employed. A 3 mm diameter glassy carbon Metrohm 628-10 rotating disk electrode was used as the working electrode for both stationary and rotating disk experiments. The counter electrode was a flame-dried platinum wire. The reference electrode for experiments in aqueous media was a Ag/AgCl (3 M NaCl) double-junction electrode. The measured $E^{\circ\prime}$ value (vs Ag/AgCl, 3 M NaCl) was converted to the Fc/Fc^+ scale using the Fc/Fc^+ standard potential in aqueous media of 210 mV vs Ag/AgCl (3 M NaCl)[28] at 25 °C (small temperature difference is neglected). A Ag/Ag^+ (CH_3CN, 10 mM $AgNO_3$) double-junction reference electrode was used in acetonitrile, and the potentials are quoted relative to the Fc/Fc^+ potential scale, using the voltammetric oxidation of ferrocene as an external reference. The working electrode was polished with an Al_2O_3 (Buehler, 0.3 μm) slurry, rinsed with distilled water, sonicated, repolished, washed with water, ethanol, dried with a tissue, and then dried with a hot air blower before being inserted into the electrochemical cell. At all times the electrochemical cell was kept under a positive pressure of N_2.

For studies in aqueous media, unless otherwise stated, KCl (0.1 M) and the relevant buffers were used as the supporting electrolyte, and the solution also was purged with N_2 for 15 min prior to each voltammetric experiment. For experiments in CH_3CN, the electrolyte (Bu_4NPF_6) was dried overnight at 100 °C in a Schlenk tube under vacuum. The solid polyoxometalate salt was dried similarly at room temperature. The electrolyte was maintained under dry dinitrogen before dried CH_3CN was transferred from a solvent tower to the Bu_4NPF_6 via gastight syringe. The resultant CH_3CN (0.1 M Bu_4NPF_6) solution was transferred via gastight syringe to the tube containing the polyoxometalate salt. The final solution was transferred similarly to a flame-dried electrochemical cell (which had been cooled in a stream of N_2) and bubbled with dry N_2 for 15 min prior to undertaking voltammetric experiments. All voltammetric experiments were undertaken in an air-conditioned laboratory at ambient temperature (20 ± 2 °C).

The glassy carbon working electrode area (7.07×10^{-2} cm^2) was determined from the peak current value obtained for the reversible one-electron oxidation of ferrocene (Fc; 1 mM) in CH_3CN (0.1 M Bu_4NPF_6) under conditions of linear sweep voltammetry and use of the Randles−Sevcik equation[29]

$$I_p = 0.4463nF\left(\frac{nF}{RT}\right)^{1/2}AD^{1/2}\nu^{1/2}C \qquad (1)$$

where I_p is the peak current (A), n (the number of electrons in the charge-transfer process) is taken to be 1.0, A is the electrode area (cm^2), D is the diffusion coefficient (taken to be 2.3×10^{-5} cm^2 s^{-1}),[29] C is the concentration (mol cm^{-3}), ν is the scan rate (V s^{-1}), and the other symbols have their usual meanings.

Kinematic viscosities (ν_k) at 20 °C of 0.00998 cm^2 s^{-1} for aqueous (0.1 M KCl) solution,[30] and 0.00456 cm^2 s^{-1} for acetonitrile solution were used for determination of the diffusion coefficients from limiting current (I_L) values obtained from rotating disk electrode (RDE) voltammetry and use of the Levich equation.[29]

Simulations of cyclic and RDE voltammograms were carried out with DigiSim (Version 3.05) software.[31]

(26) Sawyer, D. T.; Sobkowiak, A.; Roberts, J. L. J. *Electrochemistry for Chemists*, 2nd ed.; Wiley: New York, 1995.
(27) Zhang, J.; Bond, A. M.; MacFarlane, D. R.; Forsyth, S. A.; Pringle, J. M.; Mariotti, A. W. A.; Glowinski, A. F.; Wedd, A. G. *Inorg. Chem.* **2005**, *44*, 5123.
(28) Bond, A. M.; McLennan, E. A.; Stojanovic, R. S.; Thomas, F. G. *Anal. Chem.* **1987**, *59*, 2853.
(29) Bard, A. J.; Faulkner, L. R. *Electrochemical methods: fundamentals and applications*, 2nd ed.; Wiley: New York, 2001.
(30) Lobo, V. M. M.; Quaresma, J. L. *Handbook of Electrolyte Solutions, Part A*; Elsevier: New York, 1989.
(31) *DigiSim for Windows 95*, Version 3.05; Bioanalytical Systems Inc.: West Lafayette, IN, 2000.

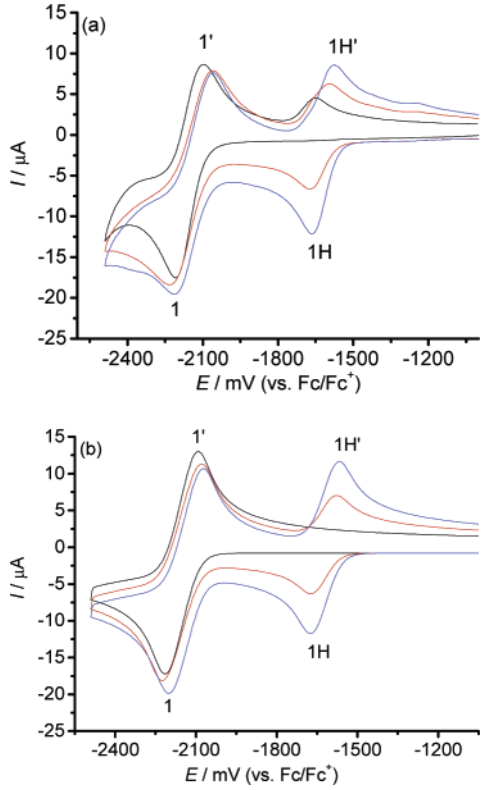

Figure 1. Comparison of experimental (a) and simulated (b) cyclic voltammograms of the $[Hept_4N]^+$ salt based upon $[\alpha\text{-}SiW_{11}O_{39}]^{8-}$ (1.56 mM) in CH_3CN (0.1 M Bu_4NPF_6). Added CF_3COOH: none (black trace); 0.38 equiv (red trace); 0.64 equiv (blue trace). Parameters used in the simulations: $A = 0.071$ cm^2, $D = 3.5 \times 10^{-6}$ cm^2 s^{-1}, $R_u = 1500$ Ohm, $C_{dl} = 8 \times 10^{-6}$ F, other parameters are listed in Table 2.

A Model 1852 TPS digital pH meter (Brisbane, Australia) equipped with an Activon ABP412 pH-probe (with a built-in Ag/AgCl, 3 M KCl reference electrode) and calibrated against standard buffers was used to determine pH values. NMR spectra were obtained with a Varian Unity Plus 400 MHz instrument in d_3-acetonitrile, with H_3PO_4 (80% in D_2O) used as an external reference for the ^{31}P NMR (set to 0 ppm). IR spectra (KBr disks) were obtained with a Bio-Rad FTS 165 FT-IR spectrometer.

Results and Discussion

Cyclic and Rotating Disk Electrode Voltammetry of $[Hept_4N]^+$ Salts in CH_3CN (0.1 M Bu_4NPF_6). Due to their extremely hygroscopic nature, these salts were isolated from toluene (see Experimental Section) and dissolved immediately in dry CH_3CN for electrochemical studies. ^1H, ^{13}C, and ^{31}P NMR spectra for the phosphate system indicated the presence of a single P-containing species in CD_3CN solution. The salts are formulated as $[Hept_4N]_8[\alpha\text{-}SiW_{11}O_{39}]$ and $[Hept_4N]_7[\alpha\text{-}PW_{11}O_{39}]$, but the exact protonation state of the anions in the $[Hept_4N]^+$ salts is unknown. Analogous $[Bu_4N]^+$ salts were formulated as $[Bu_4N]_4H_4[SiW_{11}O_{39}]$ and $[Bu_4N]_4H_3[PW_{11}O_{39}]$.[21]

System Based on $[\alpha\text{-}SiW_{11}O_{39}]^{8-}$. In aprotic media, simple one-electron steps are expected for reduction of polyoxometalate anions. Indeed, in dry acetonitrile (0.1 M Bu_4NPF_6) medium, cyclic voltammograms for this system exhibited one major well-defined process (reduction and oxidation peaks for this process are designated **1** and **1′**, respectively, in Figure 1) at very negative potentials (reversible potentials $E^{\circ\prime} = (E_p^{red} + E_p^{ox})/2$, -2155 mV vs Fc^+/Fc; $|I_p^{red}/I_p^{ox}| \approx 1$; Figure 1a; Table 1). This observation differs significantly from a report of a series of processes at less negative potentials for $[Bu_4N]_4H_4[SiW_{11}O_{39}]$.[21] However, even in our rigorously dried acetonitrile, a minor reduction process was detected prior to the major process ($E_p^{red} \approx -1721$ mV) and an oxidation process ($E_p^{ox} \approx -1650$ mV) of higher current intensity was observed on the reverse scan (Figure 1a). The current ratio $|I_p^{red}/I_p^{ox}|$ for (**1**, **1′**) under "dry" conditions was essentially independent of scan rate, but the peak-to-peak separations ΔE_p ($=E_p^{ox} - E_p^{red}$) increased from 90 to 200 mV over the scan rate range of 20−1000 mV s^{-1}. This dependence of ΔE_p on the scan rate is attributed to both the presence of uncompensated solution resistance and slow electron transfer. Processes (**1**,**1′**) (Figure 1a) are assigned to the $[SiW_{11}O_{39}]^{8-/9-}$ couple.

The relative prominence of the minor reduction processes prior to the major one and the oxidation peak at -1650 mV on the reverse scan were enhanced by deliberate addition of water. This observation implied that these processes may be a direct consequence of the presence of adventitious water and/or protons present in the synthesized $[Hept_4N]^+$ salt of $[SiW_{11}O_{39}]^{8-}$. If water present in CH_3CN provides a proton source, conditions generated are equivalent to nonbuffered media, and not to the buffered conditions commonly used in studies in aqueous media. Thus, a series of processes based on reduction of $[SiW_{11}O_{39}]^{8-}$ and protonated forms can be expected, as shown theoretically and experimentally in ref 32.

When CF_3COOH (0.38 equiv) was added to the solution, a well-defined chemically reversible process (reduction and oxidation peaks designated as **1H** and **1H′**, respectively, in Figure 1; $E^{\circ\prime} = -1633$ mV) was observed at a significantly less negative potential than that of (**1**, **1′**). The oxidation component **1H′** of this process occurred at a similar potential to that found on the reverse scan of cyclic voltammograms in "dry" acetonitrile. Consequently, it is attributed to the reduction of a protonated anion, represented by $[SiW_{11}O_{38}(OH)]^{7-}$. This simplified notation is used although the anion represented by $[SiW_{11}O_{39}]^{8-}$ may already be protonated. Since the conditions are unbuffered, individual processes are predicted to be detected for the reduction of each species present. Hence, the two resolved processes (**1**,**1′**) and (**1H**,**1H′**) observed are assigned to the couples $[SiW_{11}O_{39}]^{8-/9-}$ and $[SiW_{11}O_{38}(OH)]^{7-/8-}$.[32] In the previous study of $[Bu_4N]_4H_4[SiW_{11}O_{39}]$, three reduction processes were observed (Table 1).[21] The $E^{\circ\prime}$ value for the more negative process is similar to (**1**,**1′**), and the $E^{\circ\prime}$ value for the second process is similar to (**1H**,**1H′**) seen here in the presence of added CF_3COOH and assigned tentatively to the couple $[SiW_{11}O_{38}(OH)]^{7-/8-}$. On this basis, the third reduction process observed for $[Bu_4N]_4H_4[SiW_{11}O_{39}]$ may be associated with reduction of more highly protonated species, originating from dissolution of the latter salt with its stoichiometric protons.

(32) Guo, S.-X.; Feldberg, S. W.; Bond, A. M.; Callahan, D. L.; Richardt, P. J. S.; Wedd, A. G. *J. Phys. Chem. B* **2005**, *109*, 20641 and references therein.

Table 1. Comparison of Voltammetric Data (mV) for the Reduction of the $[Hept_4N]^+$ Salt Based upon $[\alpha\text{-}SiW_{11}O_{39}]^{8-}$ (1.56 mM) in CH_3CN (0.1 M Bu_4NPF_6) with and without Added CF_3COOH (0.64 equiv), and Data Reported in Reference 21, as Well as the Data for $[Bu_4N]_4[\alpha\text{-}SiW_{12}O_{40}]$ from Reference 9

		processes						
complex	medium	$E^{\circ\prime}$	ΔE_p	$E^{\circ\prime}$	ΔE_p	$E^{\circ\prime}$	ΔE_p	ref
$[SiW_{11}O_{39}]^{8-}$	CH_3CN	−	−	−	−	−2155	110	this work
	CH_3CN + acid[a]	−	−	−1615	80	−2135	155	
	CH_3CN[b]	−1146	124	−1653	124	−2313	121	21
$[SiW_{12}O_{40}]^{4-}$	CH_3CN	−1090	80	−1600	80	−2285	90	9

[a] $E^{\circ\prime}$ (reversible potential = $(E_p^{ox} + E_p^{red})/2$, mV), $\Delta E_p = E_p^{ox} - E_p^{red}$ (mV) (taken from cyclic voltammetry, $\nu = 100$ mV s^{-1}). [b] Data from ref 21 for $[Bu_4N]_4H_4[SiW_{11}O_{39}]$. $E^{\circ\prime}$ values are corrected from vs Ag/Ag^+ to the Fc/Fc^+ scale using a potential difference of −89 mV at 25 °C.[37]

Scheme 1

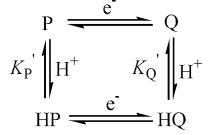

Scheme 2

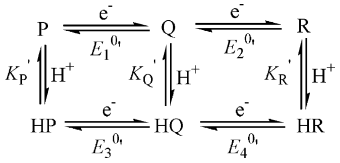

RDE voltammograms for $[SiW_{11}O_{39}]^{8-}$ (1.56 mM) in dry CH_3CN (0.1 M Bu_4NPF_6) exhibited one reduction process only for rotation rates in the range of 52.35−314.16 rad s^{-1}. A plot of I_L vs $\omega^{1/2}$ for this process was linear, indicating that a mass transport-controlled reaction occurs in the limiting current region. A plot of E vs $\ln[(I_L - I)/I]$ was linear at a rotation rate of 52.35 rad s^{-1} and an estimate of $n = 1.1$ (±0.2) was obtained from the slope (RT/nF). These data are consistent with a one-electron reduction:

$$[SiW_{11}O_{39}]^{8-} + e^- \rightleftharpoons [SiW_{11}O_{39}]^{9-} \qquad (2)$$

A diffusion coefficient (D) of 3.5 (±0.3) × 10^{-6} cm^2 s^{-1} was calculated by direct application of the Levich equation. The simple reduction mechanism of eq 2 and the experimental $E^{\circ\prime}$ value were used to simulate the RDE voltammograms. A diffusion coefficient of 3.5 (±0.1) × 10^{-6} cm^2 s^{-1} was obtained and used in the simulation of cyclic voltammograms.

The $E^{\circ\prime}$ values obtained from the present experimental data (Table 1) are much more negative than those observed for the Keggin anion $[\alpha\text{-}SiW_{12}O_{40}]^{4-}$ in CH_3CN (0.1 M Bu_4NPF_6).[9] The lower anionic charge for this anion is the likely reason for the easier reduction.

In the absence of a proton source, the reduction scheme is simply governed by the process P + $e^- \rightleftharpoons$ Q (eq 2; Scheme 1). If P = $[SiW_{11}O_{39}]^{8-}$ is present in bulk solution along with a low level of a proton source, the simple square reaction scheme of Scheme 1 might be expected to represent the voltammetric behavior. However, simulations based upon these assumptions predicted that, as the concentration of added acid increases, the current magnitude for process **1H** should increase while that for process **1** should decrease. Figure 1a demonstrates that the current associated with process **1H** increased with increasing acid concentration but that for process **1** did not decrease significantly. To accommodate the experimental observations, a double square scheme (Scheme 2) was explored in the simulation of the cyclic voltammograms, where P, Q, and R represent $[SiW_{11}O_{39}]^{8-}$, $[SiW_{11}O_{39}]^{9-}$, and $[SiW_{11}O_{39}]^{10-}$, respectively, HP, HQ, and HR represent $[SiW_{11}O_{38}(OH)]^{7-}$, $[SiW_{11}O_{38}(OH)]^{8-}$, and $[SiW_{11}O_{38}(OH)]^{9-}$, respectively, while K_P', K_Q', and K_R' are the relevant acid dissociation constants in CH_3CN.

Simulations assumed the experimental $E^{\circ\prime}$ values for processes (**1**,**1′**) and (**1H**,**1H′**) applied to reduction of P and HP, respectively. The experimental D value from RDE voltammetry was assumed for each of the anions of Scheme 2. The heterogeneous rate constants $k^{\circ\prime}$ were allowed to vary until the best fit was obtained. Since the acid dissociation constant for K_P' in CH_3CN is not available, its value was set initially at 1.0×10^{-5} M and allowed to vary until the best fit to the experimental data was obtained ($K_P' = 5.0 \times 10^{-7}$ M). The $E_4^{\circ\prime}$ value for reaction HQ + $e^- \rightleftharpoons$ HR was set initially at the same value as that for reaction P + $e^- \rightleftharpoons$ Q, while that for reaction Q + $e^- \rightleftharpoons$ R was set initially at $E_2^{\circ\prime} = E_4^{\circ\prime} - (E_3^{\circ\prime} - E_1^{\circ\prime})$. The values of $E_2^{\circ\prime}$ and $E_4^{\circ\prime}$ were then varied until the best fit was obtained. Thermodynamically allowed cross-reactions were neglected. The final simulated voltammograms in Figure 1b reflected all of the key features of the experimental ones (Figure 1a). Values of parameters used in these simulations are contained in the caption to Figure 1 and in Table 2.

System Based on $[\alpha\text{-}PW_{11}O_{39}]^{7-}$. At slow scan rates, cyclic voltammograms in dry CH_3CN (0.1 M Bu_4NPF_6) exhibited just one major chemically reversible reduction process in the potential range available (see peaks **1** and **1′** in Figure 2a). This observation again differs significantly from a report of a series of processes at less negative potentials for $[Bu_4N]_4H_3[PW_{11}O_{39}]$.[21] However, even in our rigorously dried acetonitrile, a minor reduction process was detected prior to the major process (Figure 2a). The current ratio $|I_p^{red}/I_p^{ox}|$ for (**1**,**1′**) at −1757 mV under "dry" conditions was essentially independent of scan rate. This reaction was assigned to a one-electron process:

$$[PW_{11}O_{39}]^{7-} + e^- \rightleftharpoons [PW_{11}O_{39}]^{8-} \qquad (3)$$

The $E^{\circ\prime}$ value of −1757 mV was significantly less negative than that for $[\alpha\text{-}SiW_{11}O_{39}]^{8-/9-}$ (Table 3). This difference is

Table 2. Key Parameters Used to Simulate Cyclic Voltammograms Presented in Figure 1b

Electron-Transfer Reactions	$E^{\circ\prime}$/mV	$k^{\circ\prime}$ [b]/ cm s^{-1}
$[SiW_{11}O_{39}]^{8-} + e^- \rightleftharpoons [SiW_{11}O_{39}]^{9-}$	−2150	$\geq 5.0 \times 10^{-2}$
$[SiW_{11}O_{39}]^{9-} + e^- \rightleftharpoons [SiW_{11}O_{39}]^{10-}$	(-2650 ± 100)[c]	$\geq 5.0 \times 10^{-2}$
$[SiW_{11}O_{38}(OH)]^{7-} + e^- \rightleftharpoons [SiW_{11}O_{38}(OH)]^{8-}$	−1620	$\geq 5.0 \times 10^{-2}$
$[SiW_{11}O_{38}(OH)]^{8-} + e^- \rightleftharpoons [SiW_{11}O_{38}(OH)]^{9-}$	−2120	$\geq 5.0 \times 10^{-2}$

Chemical Reactions	K/M	k_f/s^{-1}	$k_b/M^{-1}\ s^{-1}$
$[SiW_{11}O_{38}(OH)]^{7-} \rightleftharpoons [SiW_{11}O_{39}]^{8-} + H^+$	K_P', 5.0×10^{-7}	5.0×10^3	1.0×10^{10}
$[SiW_{11}O_{38}(OH)]^{8-} \rightleftharpoons [SiW_{11}O_{39}]^{9-} + H^+$	K_Q', 3.9×10^{-16}	3.9×10^{-6}	1.0×10^{10}
$[SiW_{11}O_{38}(OH)]^{9-} \rightleftharpoons [SiW_{11}O_{39}]^{10-} + H^+$	K_R', 3.0×10^{-25}	3.0×10^{-15}	1.0×10^{10}

[a] The parameters used in the simulation are based on the formula: $[Hept_4N]_8[SiW_{11}O_{39}]\cdot 3Hept_4NBr\cdot 2KCl$. [b] Values of $k^{\circ\prime}$ can be varied from 5.0×10^{-2} to 1.0×10^4 cm s^{-1} without affecting the simulated voltammograms. [c] The absolute value in parentheses is not significant to outcome of simulation.

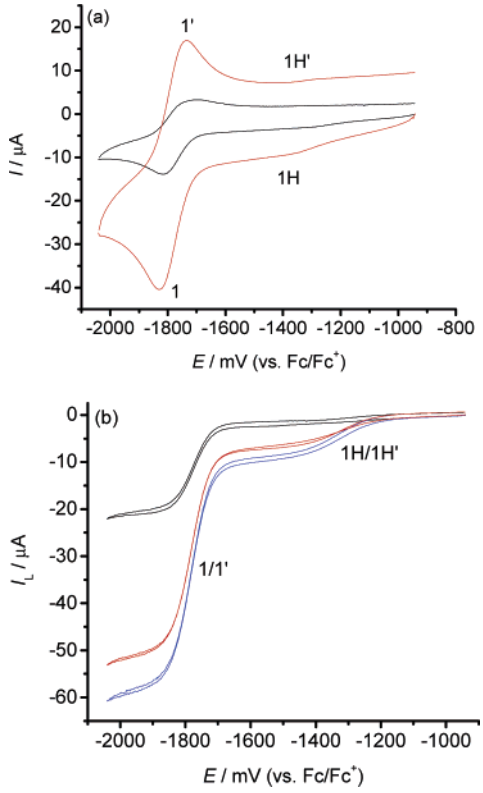

Figure 2. Cyclic (a) and RDE (b) voltammograms of the $[Hept_4N]^+$ salt based upon $[\alpha\text{-}PW_{11}O_{39}]^{7-}$ (2 mM) in CH_3CN (0.1 M Bu_4NPF_6). (a) scan rate: 100 (black trace) and 1000 mV s^{-1} (red trace); (b) scan rate: 10 mV s^{-1}, rotation rates: 52.35 (black trace), 261.8 (red trace), and 314.16 rad s^{-1} (blue trace).

expected due to the lower anionic charge of $[PW_{11}O_{39}]^{7-}$ allowing easier reduction (Table 3).[3] This value is much more negative than that for the $[PW_{12}O_{40}]^{3-/4-}$ process in CH_3CN (−669 mV),[9] again consistent with the expectation that lower anionic charges allow easier reduction.[3]

A minor reduction process at about −1290 mV became more prominent when the scan rate was increased (see peaks **1H** and **1H′** in Figure 2a), implying that it is derived from a kinetically controlled step coupled to the $[PW_{11}O_{38}(OH)]^{6-/7-}$ charge-transfer process. As for the $[SiW_{11}O_{39}]^{8-}$ system, this process is likely to be derived from protons present in the $[Hept_4N]^+$ salts or formed from adventitious water present in "dry" acetonitrile. The relative prominence of process **1H** also was enhanced by addition of water or CF_3COOH, supporting the hypothesis that it is associated with the reduction of a protonated species. The process tentatively associated with reduction of $[PW_{11}O_{38}(OH)]^{6-}$ also became more prominent in RDE voltammograms as the rotation rate increased (Figure 2b), again consistent with the presence of kinetic control. Two reduction processes were observed for $[Bu_4N]_4H_3[PW_{11}O_{39}]$ in MeCN.[21] The $E^{\circ\prime}$ value for the second process in this report (ref 21) is close to that obtained as the major process in "dry" CH_3CN in the present work (Table 3). The data in ref 21 are consistent with the presence of protons in that system. Simulation of this inherently very complex kinetically controlled system was not undertaken.

Voltammetry of $[\alpha\text{-}SiW_{11}O_{39}]^{8-}$ in Buffered Aqueous Media. Cyclic and Rotating Disk Voltammetry at pH 4.6 (Potassium Acetate Buffer + 0.1 M KCl). A cyclic voltammogram of $[\alpha\text{-}SiW_{11}O_{39}]^{8-}$ (1 mM) obtained at a glassy carbon electrode in buffered aqueous medium at pH 4.6 containing 0.1 M KCl electrolyte is shown in Figure 3a. Two reduction processes with reversible potentials, $E^{\circ\prime}$, of −882 (process **I**) and −1081 mV (process **II**) vs Fc/Fc^+ respectively, are observed (Table 5). These potentials are consistent with literature values reported in buffered aqueous media at pH 4.7, where these two processes are assigned to two overall $2e^-$ redox couples.[12,23,33] The peak-to-peak separations, ΔE_p, increased from 41 to 66 mV for the first reduction process and from 53 to 66 mV for the second process in the scan rate range of 20−1000 mV s^{-1}. For a simple electrochemically reversible process involving the transfer of n electrons, the predicted value of $\Delta E_p = 56/n$ mV at 293 K is expected to be independent of scan rates.[29] The observed slight dependence of ΔE_p on scan rate is consistent with overall $2e^-$ charge transfer steps with chemical reactions coupled to the electron transfer processes. These complications may be attributed either to the electron transfer being slow on the electrochemical time scale or to proton-coupled processes becoming kinetically controlled under higher-scan-rate conditions. The scan rate dependence is unlikely to be a result of uncompensated resistance in the electrochemical cell, as the latter is small in the aqueous medium used.

Figure 3b demonstrates that reduction of $[\alpha\text{-}SiW_{11}O_{39}]^{8-}$ at pH 4.6 at a rotating disk GC electrode also occurred via two sigmoidal-shaped reduction steps (processes **I** and **II**). The experimental ratios of the limiting currents, I_L, are close

(33) Kim, J.; Gewirth, A. A. *Langmuir* **2003**, *19*, 8934.

Table 3. Comparison of Voltammetric Data (mV) for the Reduction of the $[Hept_4N]^+$ Salt Based upon $[\alpha\text{-}PW_{11}O_{39}]^{7-}$ (2 mM) in CH_3CN (0.1 M Bu_4NPF_6), the Data for $[Bu_4N]_4H_3[\alpha\text{-}PW_{11}O_{39}]$ from Reference 21, and the Data for $[\alpha\text{-}PW_{12}O_{40}]^{3-}$ from Reference 9[a]

	processes								
complex	$E^{\circ\prime}$	ΔE_p	$E^{\circ\prime}$	ΔE_p	$E^{\circ\prime}$	ΔE_p	$E^{\circ\prime}$	ΔE_p	ref
$[PW_{11}O_{39}]^{7-}$	–	–	–	–	–	–	−1757	120	this work
	–	–	–	–	−1194	91	−1727	128	21
$[PW_{12}O_{40}]^{3-}$	−669	73	−1186	74	−1894	74	−2397	78	9

[a] $E^{\circ\prime}$ (reversible potential $= (E_p^{ox} + E_p^{red})/2$, mV), $\Delta E_p = E_p^{ox} - E_p^{red}$ (mV) (taken from cyclic voltammetry, $\nu = 100$ mV s^{-1}). Data from ref 21 for $[Bu_4N]_4H_3[\alpha\text{-}PW_{11}O_{39}]$. $E^{\circ\prime}$ values are corrected from the Ag/Ag^+ to the Fc/Fc^+ scale using a potential difference of −89 mV at 25 °C.[37]

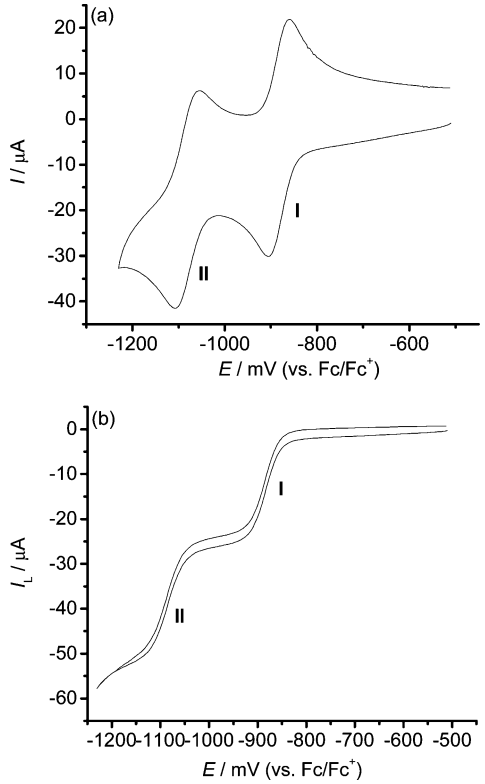

Figure 3. Cyclic (a) and RDE (b) voltammograms of 1 mM $[\alpha\text{-}SiW_{11}O_{39}]^{8-}$ obtained at a glassy carbon electrode in buffered aqueous solution (0.1 M potassium acetate + 0.1 M KCl) at pH 4.6. Scan rates: 100 (a) and 10 mV s^{-1} (b). Rotation rate: 52.35 rad s^{-1}.

Table 4. Comparison of the Voltammetric Data (mV) Obtained by Cyclic Voltammetry at a Scan Rate of 100 mV s^{-1} for Reduction of $[\alpha\text{-}SiW_{12}O_{40}]^{4-}$ and $[\alpha\text{-}SiW_{11}O_{39}]^{8-}$ in Buffered Aqueous Media

	$[\alpha\text{-}SiW_{12}O_{40}]^{4-}$						$[\alpha\text{-}SiW_{11}O_{39}]^{8-}$			
	process **I**		process **II**		process **III**		process **I**		process **II**	
pH	$E^{\circ\prime}$	ΔE_p	$E^{\circ\prime}$	ΔE_p	$E^{\circ\prime}$	ΔE_p	$E^{\circ\prime}$	ΔE_p	$E^{\circ\prime}$	ΔE_p
2.1	−421	71	−680	72	−958	46	−703	44	−911	49
2.9							−754	44	−957	51
3.1							−773	44	−978	54
3.8							−820	46	−1025	54
4.2							−850	47	−1056	54
4.6	−409	76	−668	70	−1114	88	−882	49	−1081	56
6.0	−417	74	−677	71	−1108	92	−975	51	−1181	78
6.8	−410	82	−665	81	−1091	120			−1258	156

[a] See Experimental Section for specific details of buffers.

to unity (Table 5), and the half-wave potentials, $E_{1/2}$ (E at $I_L/2$), for **I** and **II** are −881 and −1082 mV, respectively, consistent with the $E^{\circ\prime}$ values obtained from cyclic voltammetry. Plots of I_L vs $\omega^{1/2}$ for both processes **I** and **II** were linear, indicating the presence of mass transport-controlled reactions in the limiting current region.[29] A diffusion coefficient (D) of 2.6 (±0.3) × 10^{-6} cm^2 s^{-1} was calculated by application of the Levich equation,[29] assuming the electron-transfer number, n, is 2.

The proximity of processes **I** and **II** means that the current in the potential region between them is sloped, making accurate calculation of I_L (and hence, of D) values difficult. However, an accurate value of I_L could be achieved by inclusion of the contributions from all processes in the simulation.[32] Consequently, the simple scheme A + $2e^- \rightleftharpoons$ B, B + $2e^- \rightleftharpoons$ C was simulated, with each process assumed to be a simple quasi-reversible reaction (with a single reversible potential, E_{app}', heterogeneous charge-transfer rate constant, k_{app}', and charge-transfer coefficient, α, of 0.5). Each species was assumed to have the same diffusion coefficient, D. Coupled chemical reactions associated with process **I** and **II** were not included in this initial simulation but were accommodated in later simulations. Simulation of the RDE data according to this simplified scheme and application of the autofitting function available with the DigiSim[31] software led to an estimation of $D = 2.8$ (±0.1) × 10^{-6} cm^2 s^{-1} at pH 4.6, a value consistent with that (2.6 (±0.3) × 10^{-6} cm^2 s^{-1}) obtained by direct use of the Levich equation (see above). This value of D was used in all subsequent simulations.

The reversible potentials for the first two reduction processes of the lacunary anion $[\alpha\text{-}SiW_{11}O_{39}]^{8-}$ (−881 and −1082 mV, respectively) are considerably more negative than those observed for its parent Keggin anion $[\alpha\text{-}SiW_{12}O_{40}]^{4-}$ (−409 and −668 mV, respectively) at pH 4.6 (Table 4). Its high negative formal charge means that $[SiW_{11}O_{39}]^{8-}$ is likely to be more basic and more difficult to reduce than $[\alpha\text{-}SiW_{12}O_{40}]^{4-}$. It is known to bind three protons (pK_a 5.19, 4.0, and 1.6) to form $[SiW_{11}O_{36}(OH)_3]^{5-}$ in acidic aqueous solution and to associate with monovalent cations.[19,20] Therefore, the effects on the electrochemistry of both proton concentration and those of the monovalent cations present in the buffers need to be understood.

Effect of Cations and Ionic Strength. The formal anionic charge on $[\alpha\text{-}SiW_{11}O_{39}]^{8-}$ is much greater than that of ions such as $[Fe(CN)_6]^{4-}$ that are known to form ion pairs with alkali cations. Consequently, $[\alpha\text{-}SiW_{11}O_{39}]^{8-}$ is likely to form ion pairs with the cations of the supporting electrolyte. The effect of cation concentration on the voltammetry was obtained for solutions of $[SiW_{11}O_{39}]^{8-}$ (1 mM) in acetate buffer solutions at pH 4.6 containing K^+ or Na^+ at variable

Table 5. Comparison of the Influence of Variation of Cations and Ionic Strength on the Voltammetry of $[\alpha\text{-SiW}_{11}O_{39}]^{8-}$ (1 mM) Obtained at a Glassy Carbon Electrode (d = 3 mm) in Buffered Aqueous Media at pH 4.6

medium[a]			process **I**			process **II**		
cation	cation added to buffer	total cation concn[b] (M)	$E^{\circ\prime}$ (mV)	ΔE_p (mV)	I_L (μA)	$E^{\circ\prime}$ (mV)	ΔE_p (mV)	I_L (μA)
Na^+	–	0.10	−891	78	21.0	−1094	76	23.0
Na^+ (1M)	–	1.0	−940	78	16.8	−1072	79	20.0
Na^+	Na^+	0.20	−891	55	20.0	−1080	56	25.0
Na^+	K^+	0.20	−899	56	24.0	−1085	56	27.0
Na^+	Na^+ (1 M)	1.1	−929	71	7.0	−1087	66	20.0
K^+	–	0.10	−884	53	25.0	−1089	59	26.0
K^+	Na^+	0.20	−893	54	22.0	−1079	54	27.0
K^+	K^+	0.20	−882	46	25.0	−1081	54	27.0
K^+	Na^+ (1 M)	1.1	−914	70	15.0	−1062	53	26.0

[a] The concentrations of acetate buffer and chloride salt are both 0.1 M unless otherwise stated. [b] Proton concentrations are neglected. [c] $E^{\circ\prime}$ (reversible potential = $(E_p^{ox} + E_p^{red})/2$, mV), $\Delta E_p = E_p^{ox} - E_p^{red}$ (mV) (taken from cyclic voltammetry, ν = 100 mV s^{-1}), I_L, μA (taken from RDE experiments, rotation rate: 52.35 rad s^{-1}, ν = 10 mV s^{-1}).

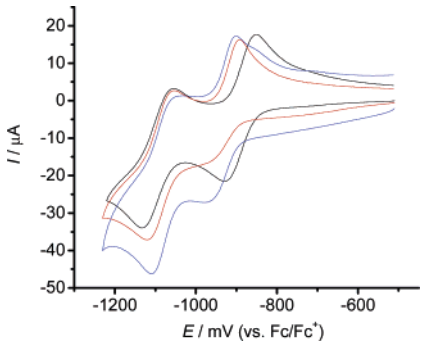

Figure 4. Comparison of cyclic voltammograms of 1 mM $[\alpha\text{-SiW}_{11}O_{39}]^{8-}$ at pH 4.6 obtained in 0.1 M sodium acetate (black), 0.1 M sodium acetate + 1 M NaCl (red) and 1 M sodium acetate buffer (blue). Scan rate: 100 mV s^{-1}.

concentrations. The results are summarized in Table 5 and Figure 4. Process **I** is affected significantly, but not process **II**.

Cyclic and RDE voltammograms (Table 5) obtained in 0.1 M buffer containing K^+ cation are similar to those obtained in buffer containing 0.1 M Na^+ cation, but with notably smaller values of ΔE_p. When the concentration of sodium acetate buffer was increased from 0.1 to 1 M, the potential of the first reduction process shifted to a more negative value (Table 5, Figure 4), the wave shape changed, and the RDE limiting current decreased. The effect of Na^+ is even more pronounced when 1 M NaCl is added to the 0.1 M sodium acetate buffer (see Figure 4 and Table 5). Replacement of Na^+ by K^+ produced relatively minor changes at the 0.1 M concentration level (see Table 5). Thus, the major impact is at very high ionic strength where process **I** was greatly diminished in current and became subject to kinetic control. The effect of high K^+ concentration could not be explored due to precipitation of polyoxometalate salts. In summary, at pH 4.6, differences due to the presence of Na^+ or K^+ at the 0.1 M level are relatively small, implying the thermodynamics are predominantly governed by H^+. However, at high 1 M NaCl ionic strength, the kinetics are altered and the first process is no longer diffusion (mass transport) controlled. Consequently, subsequent studies use 0.1 M KCl to control the ionic strength, and it is assumed that the kinetics and thermodynamics are dominated by H^+ so that ion-pairing effect from K^+ can be neglected.

Influence of Proton Concentration. The above studies on the medium effect implied that use of a buffer to which 0.1 M NaCl or 0.1 M KCl has been added provides conditions where the influence of Na^+ or K^+ ion-pairing is small relative to that of H^+ bonding to the oxo framework of the anion and where establishment of acid−base equilibria is fast, allowing diffusion control to dominate. Studies on the pH dependence were carried out in the presence of 0.1 M KCl. Under such conditions, two $2e^-$ reduction processes were observed in the cyclic voltammogram of $[\alpha\text{-SiW}_{11}O_{39}]^{8-}$ (1 mM) at pH 2.1 (0.01 M HCl + 0.1 M KCl). Two processes were also present in buffered media at pH 4.6 (Figure 5), but they were detected at less negative potentials under the more acidic conditions (Table 4). A minor anodic process was observed between the two main waves at scan rates ≤500 mV s^{-1}. This additional process has been attributed to the generation of the β isomer (reduced form),[15] which is known to be reduced at more positive potentials than the corresponding α isomer.[1] This particular process was neglected in simulations of the voltammetry. Data obtained over the pH range of 2.1−6.8 are summarized in Table 4.

In the pH range 2.1−4.6, both processes shifted negatively with increasing pH. However, at pH 6.0 and 6.8 where protons are less available, a significant change in the wave shape occurred for process **I**. This change is similar to that observed at pH 4.6 at very high Na^+ concentrations (Figure 4). It is assumed that ion-pairing with Na^+ or K^+ becomes significant under conditions where the H^+ concentration is low because the full negative charge of the anion emerges.

When reduction of species Ox to Red is coupled with proton-transfer steps, the overall reaction can be written as

$$\mathrm{Ox} + ne^- + m\mathrm{H}^+ \rightleftharpoons \mathrm{Red} \qquad (4)$$

If all steps are reversible (for details, see ref 9):

$$E_{\mathrm{measured}}{}^{\circ\prime} = E^{\circ\prime} - (RT/nF)\ln\{[\mathrm{Red}]/[\mathrm{Ox}]\} - (2.303mRT/nF)\ \mathrm{pH} \qquad (5)$$

eq 5 indicates that the difference in the numbers of protons

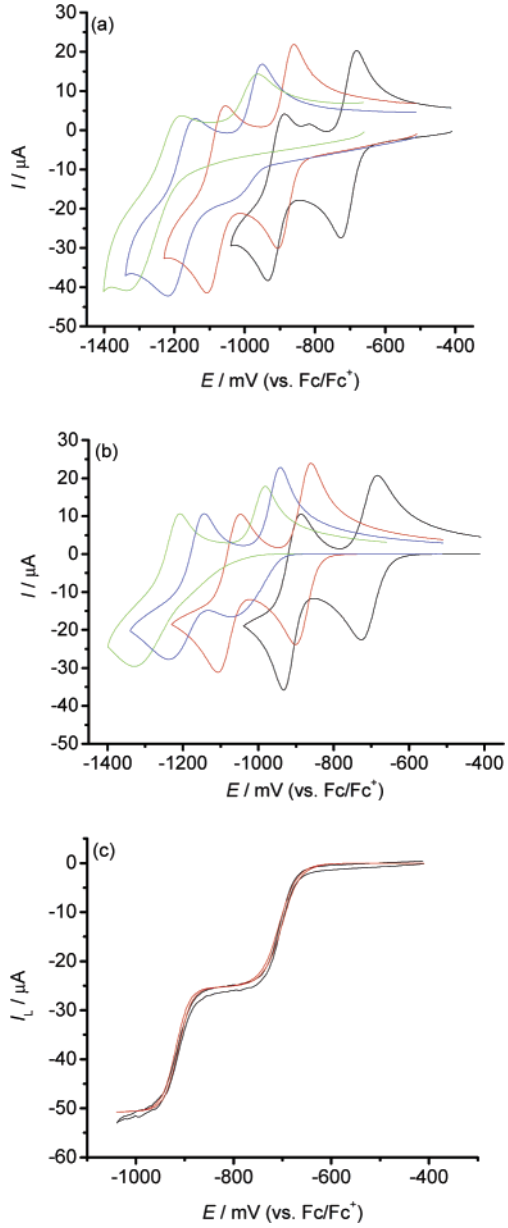

Figure 5. Comparison of experimental (a) and simulated (b) cyclic voltammograms of $[\alpha\text{-SiW}_{11}O_{39}]^{8-}$ (1 mM) in buffered media. Parameters used in the simulation are as summarized in Table S1 and described in the text. pH 2.1 (black), 4.6 (red), 6.0 (blue), and 6.8 (green). Scan rate: 100 mV s^{-1}. (c) Comparison of experimental (black) and simulated (red) RDE voltammograms of $[\alpha\text{-SiW}_{11}O_{39}]^{8-}$ (1 mM) in buffered medium at pH 2.1, scan rate: 10 mV s^{-1}, rotation rate: 52.35 rad s^{-1}.

transferred when Ox is converted to Red (m) can be calculated by plotting $E_{measured}{}^{\circ\prime}$ (V) vs pH and obtaining the slope $= -2.303mRT/nF$.

Such plots for the range when the processes are close to reversible are shown in Figure 6a. Assuming $n = 2$, the difference in the numbers of protons involved (m) in each process was calculated to be 2.4 for process **I** and 2.5 for process **II**, i.e., m lies between 2 and 3. Souchay et al. have reported analogous plots using polarographic data but under different conditions.[16] The nonintegral values imply a series of acid−base equilibria may contribute to $E_{measured}{}^{\circ\prime}$.

Under RDE conditions (Figure 6b), the experimental ratios of the limiting currents, I_L, for the two reduction processes

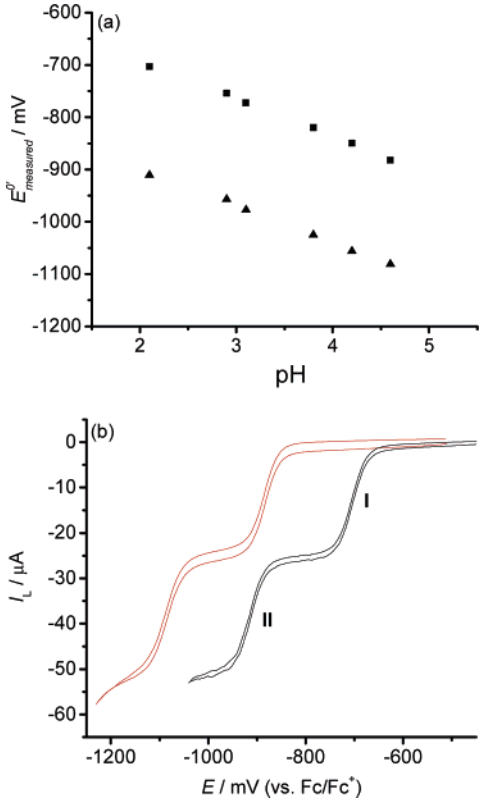

Figure 6. (a) Plots of $E_{measured}{}^{\circ\prime}$ vs pH for both reduction processes of $[SiW_{11}O_{39}]^{8-}$ (1 mM) in the pH range 2.1−4.6. (■) process **I**, (▲) process **II**. (b) RDE voltammograms of $[SiW_{11}O_{39}]^{8-}$ (1 mM) at pH 2.1 (black) and 4.6 (red). Scan rate: 10 mV s^{-1}, rotation rate: 52.35 rad s^{-1}.

are unity over the pH range 2.1−4.6. The half-wave potentials $E_{1/2}$ (E at $I_L/2$) for **I** and **II** shifted to more negative values with increasing pH over this pH range and for rotation rates 52.35−314.16 rad s^{-1}. These results are consistent with the cyclic voltammetric data. At the higher pH values studied of 6.0 and 6.8, I_L for process **I** became diminished and this process is no longer mass transport controlled under these less acidic conditions.

Equation 5 requires equilibrium conditions to be present. Rigorous descriptions of electrode processes involving extensive acid−base and ion-pairing chemistry are complex, as kinetically and not thermodynamically controlled conditions are likely to apply. Consequently, considerations of heterogeneous kinetics and thermodynamics of the individual electron transfer steps are required, as well as the homogeneous kinetics and thermodynamics of the protonation and ion-pairing processes. Simulations are usually required to probe the details of such complex mechanisms.

To simplify the simulations, ion-pairing with K^+ was neglected in the present study. All homogeneous rate constants for protonation were assumed to be diffusion controlled and set at a value of 1.0×10^{10} M^{-1} s^{-1}. Furthermore, all charge-transfer coefficients (α) were assumed to be 0.5. In contrast, the heterogeneous rate constants for electron transfer were adjusted until the best fits to data were obtained. It is obviously sensible to include as many independently known parameters as possible into this complex simulation. However, it was not possible in this study to obtain independently the individual $E°$ and $k°$ values

Scheme 3

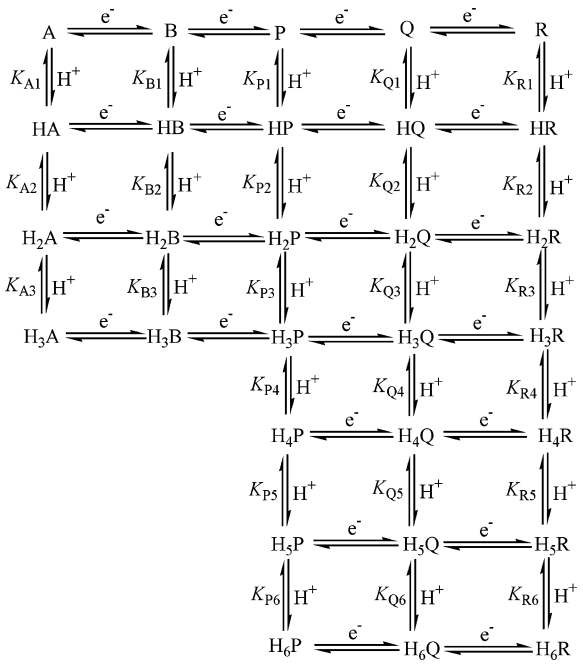

for each 1e$^-$ electron transfer processes nor the homogeneous kinetics and thermodynamics of most of the protonation processes. Thus, in principle and probably in practice, the mechanism is very complex and involves too many adjustable parameters to obtain a quantitative evaluation of all steps that are included in Scheme 3.

The pH-dependence of the voltammetry of $[\alpha\text{-}SiW_{12}O_{40}]^{4-}$ is simpler than for that of $[\alpha\text{-}SiW_{11}O_{39}]^{8-}$ with its higher formal charge. The first two processes for $[\alpha\text{-}SiW_{12}O_{40}]^{4-}$ are independent of pH, while the reversible potential for the third process **III** (associated with the couple $[SiW_{12}O_{40}]^{6-/7-}$) reaction shifts -60 mV per pH unit in the pH range 2.1−4.6 and then remains independent of pH in the range 4.6−6.8. In contrast, the reversible potentials for processes **I** and **II** of $[SiW_{11}O_{39}]^{8-}$ shift -68 mV per pH unit over the pH range 2.1−4.6, with kinetic control being detected at higher pH values. However, the ladder-square scheme established for process **III** of $[SiW_{12}O_{40}]^{4-}$ could be used as the initial basis for simulation of processes **I** and **II** of $[SiW_{11}O_{39}]^{8-}$ (Figures 5, 6).[9] Knowing $n = 2$, $m = 2.4$, and that $[SiW_{11}O_{39}]^{8-}$ can bind three protons,[19] the following ladder-square Scheme 4 was proposed for the first reduction process, where: A, B, and P represent $[SiW_{11}O_{39}]^{8-}$, $[SiW_{11}O_{39}]^{9-}$, and $[SiW_{11}O_{39}]^{10-}$, respectively; HA, H_2A, and H_3A are $[SiW_{11}O_{38}(OH)]^{7-}$, $[SiW_{11}O_{37}(OH)_2]^{6-}$, and $[SiW_{11}O_{36}(OH)_3]^{5-}$; HB, H_2B, and H_3B are $[SiW_{11}O_{38}(OH)]^{8-}$, $[SiW_{11}O_{37}(OH)_2]^{7-}$, and $[SiW_{11}O_{36}(OH)_3]^{6-}$; HP, H_2P, and H_3P are $[SiW_{11}O_{38}(OH)]^{9-}$, $[SiW_{11}O_{37}(OH)_2]^{8-}$, and $[SiW_{11}O_{36}(OH)_3]^{7-}$, respectively. p$K_{A1}$, p$K_{A2}$, and p$K_{A3}$ correspond to the three pK_a values of $[SiW_{11}O_{39}]^{8-}$, which are 5.19, 4.0, and 1.6, respectively,[19] and are defined in eq 6 for the reaction: HA ⇌ A + H$^+$ ($k_{f,A}$, $k_{b,A}$, where $k_{b,A} = 1.0 \times 10^{10}$ M^{-1} s^{-1}).

$$K_A = (a_{H^+}[A]/[HA]) = \frac{k_{f,A}}{k_{b,A}} \quad (6)$$

The activity of H$^+$, a_{H^+} was determined from the relationship: $a_{H^+} = 10^{-pH}$. In the above equilibrium relationship (eq 6), a mixture of activity and concentration terms are employed to reflect the experimental reality that applies to the system being studied (a_{H^+} via a pH electrode and concentrations via voltammetry for polyoxometalate species).

An analogous scheme also may be proposed for process **II** as the same number of electrons and protons are involved as for process **I**. With this approach, the overall full reaction scheme to be simulated would be as given in Scheme 3.

Ideally, the $E^{\circ\prime}$ values for reactions not involving coupled proton reactions such as A + e$^-$ ⇌ B and B + e$^-$ ⇌ P should be directly measurable at high pH values and then included directly into the simulation as known values. Unfortunately, $[SiW_{11}O_{39}]^{8-}$ is unstable when the pH value is higher than 6. However, data in acetonitrile (see later) suggest that $E^{\circ\prime}$ values for these reactions are very negative. Furthermore, the separation of consecutive pairs reduction processes,[9] e.g., A + e$^-$ ⇌ B and B + e$^-$ ⇌ P; P + e$^-$ ⇌ Q and Q + e$^-$ ⇌ R are usually very similar (about 200 mV) in polyoxometalate systems. Additionally, the separation between these pairs is usually much larger than this value. Values used in the simulation comply with these general principles. Moreover, protonated polyoxometalate species are invariably easier to reduce than unprotonated species of the same redox state so that the $E^{\circ\prime}$ values for the protonated species were set in initial guesses at more positive values than those of the unprotonated species, i.e., $E^{\circ\prime}$ (H_3A/H_3B) > $E^{\circ\prime}$ (H_2A/H_2B) > $E^{\circ\prime}$ (HA/HB) > $E^{\circ\prime}$ (A/B), etc.

Once the combination of guessed $E^{\circ\prime}$ values for different electron-transfer reactions and known K_{A1}, K_{A2}, and K_{A3} values were entered into the simulation, values of K_{B1}, K_{B2}, K_{B3}, K_{P1}, K_{P2}, and K_{P3} associated with one- and two-electron reduced species are automatically defined from the $\Delta G^\circ = -RT \ln K = -F\Delta E^{\circ\prime}$ relations that apply for Scheme 4, as discussed by Feldberg et al.[34] These requisite thermodynamic constraints are automatically invoked in the DigiSim program.[31] Analogous considerations apply to these and other electron-transfer steps prescribed in Scheme 3.

In this study, the need to introduce aphysically large rate constants, i.e., second-order reactions faster than $\sim 10^{10}$ M^{-1} s^{-1} and/or first-order reactions faster than $\sim 10^{12}$ s^{-1}, was avoided by introduction of general acid−base catalysis into the simulations. The procedure for implementation of this approach, which takes advantage of the properties of a buffer, is described in detail in ref 32. Simulations based on Scheme 3 using acid−base catalysis reactions were considered using the parameters listed in Table S1, but clearly the significance of values used is variable. For example, the reduction processes involving species P, Q, R, and their one- or two-proton coupled forms occur at very negative potential (out of the potential range studied). This implies that heteroge-

(34) Rudolph, M.; Reddy, D. P.; Feldberg, S. W. *Anal. Chem.* **1994**, *66*, 589A.

Scheme 4

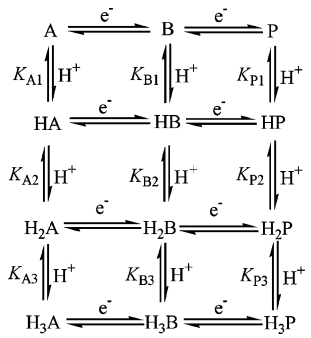

Scheme 5

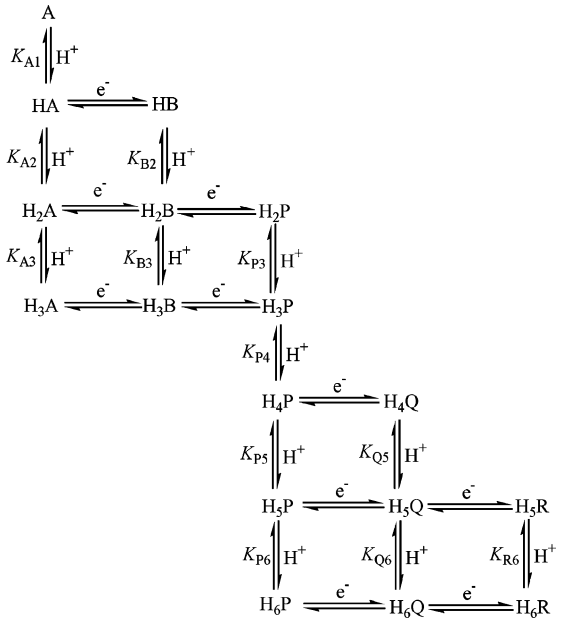

neous reactions, as well as the homogeneous chemical reactions involving these species, do not contribute significantly to the outcome of the simulation. Thus, $E^{\circ\prime}$ and k° values for designated electron-transfer reactions in Table S1 are not highly significant (they are regarded as qualitative estimates only), nor are K values for processes $[SiW_{11}O_{38}(OH)]^{9-} \rightleftharpoons [SiW_{11}O_{39}]^{10-} + H^+$ (K_{P1}), $[SiW_{11}O_{38}(OH)]^{10-} \rightleftharpoons [SiW_{11}O_{39}]^{11-} + H^+$ (K_{Q1}), $[SiW_{11}O_{38}(OH)]^{11-} \rightleftharpoons [SiW_{11}O_{39}]^{12-} + H^+$ (K_{R1}), and K_{P2}, K_{P3}, K_{Q2}, K_{Q3}, K_{R2}, K_{R3}, and other K values that are not listed in Table S1, which are defined by the requisite thermodynamic constraints automatically invoked in the DigiSim program.[31] This implies that the outcome of the simulation is dominated by terms present in Scheme 5 and that only parameters needed to define terms presented in this scheme have quantitative significance. Thus, values of K selected for processes $[SiW_{11}O_{35}(OH)_4]^{6-} \rightleftharpoons [SiW_{11}O_{36}(OH)_3]^{7-} + H^+$, $[SiW_{11}O_{34}(OH)_5]^{5-} \rightleftharpoons [SiW_{11}O_{35}(OH)_4]^{6-} + H^+$, and $[SiW_{11}O_{33}(OH)_6]^{4-} \rightleftharpoons [SiW_{11}O_{34}(OH)_5]^{5-} + H^+$ are critical to achieve a satisfactory simulation, as are the $k^{\circ\prime}$ values for the electron-transfer reactions $[SiW_{11}O_{37}(OH)_2]^{6-} + e^- \rightleftharpoons [SiW_{11}O_{37}(OH)_2]^{7-}$, $[SiW_{11}O_{35}(OH)_4]^{6-} + e^- \rightleftharpoons [SiW_{11}O_{35}(OH)_4]^{7-}$, and $[SiW_{11}O_{34}(OH)_5]^{6-} + e^- \rightleftharpoons [SiW_{11}O_{34}(OH)_5]^{7-}$, while other $k^{\circ\prime}$ values are not highly significant. It should also be noted that the formation of the β isomer of the anion was not included in the simulation. The voltammograms (Figure 5b) simulated according to Scheme 5 reflect the key features of the experimental voltammograms at all pH values examined experimentally.

Table 6. Voltammetric Data of the Reduction of $[\alpha\text{-}PW_{11}O_{39}]^{7-}$ (1 mM) in Buffered Aqueous Media

	process **I**			process **II**		
pH	$E^{\circ\prime}$ (mV)	ΔE_p (mV)	$I_L{}^a$ (mA)	$E^{\circ\prime}$ (mV)	ΔE_p (mV)	$I_L{}^a$ (mA)
2.1	−681	42	27	−890	57	27
2.9	−731	44	25	−936	57	27
3.7	−794	47	25	−987	58	27
4.2	−830	51	23	−1016	59	25
4.6	−868	55	12	−1048	61	27
6.1	−863[b]	-	-	−1166	183	43

[a] I_L, μA (taken from RDE experiments, rotation rate: 52.35 rad s^{-1}, ν = 10 mV s^{-1}). [b] This is the peak potential of the anodic wave.

In summary, the multi-square-scheme mechanism (Schemes 3 and 5) allowed the essential thermodynamic and kinetic features of this system to be captured, but the relative significance of the steps needs to be considered. As noted elsewhere,[9,32] while the set of parameters chosen for use in the simulation are all physically and chemically sensible and they enable experimental voltammograms to be mimicked satisfactorily over a wide range of scan rates and pH-values, limitations in the significance of the theory−experiment comparison need to be understood. In particular, it is found that peak potentials deduced from simulations closely match those found experimentally. In contrast, current values are more difficult to accurately mimic by simulation because of the contribution from a sloping background current and isomerization that is not included in the simulation. Details of the treatment of the background and the criteria of determining the acceptability of a simulation have been discussed in ref 9. Finally, it needs to be understood that, despite the generally good agreement between the simulated and experimental voltammograms and despite our best endeavors, in a complex mechanism of this kind containing many adjustable parameters it cannot be guaranteed that a unique solution has been obtained.

To support the fidelity of the strategy employed, RDE voltammograms were also simulated using Scheme 3 (5). Excellent agreement between experimental and simulated data was obtained under these steady-state conditions (see Figure 5c at pH 2.1) where background capacitance current is negligible.

Comparison of the $E^{\circ\prime}$ Values for $[\alpha\text{-}SiW_{11}O_{39}]^{8-}$ Obtained in Acetonitrile and Aqueous Media. The reversible potential values obtained in acetonitrile are very much more negative (more than a volt) than those obtained in aqueous media (Tables 1 and 4). This could be attributed in part to the different electrophilic properties of solvents, which is quantified by the acceptor number *AN*.[35] Thus, reduction for such a $[SiW_{11}O_{39}]^{8-/9-}$ process becomes more difficult with decreasing solvent acceptor number:[36] H_2O (54.8) >

(35) Reichardt, C. *Solvents and Solvent Effects in Organic Chemistry*, 3rd ed.; Wiley-VCH: Weinheim, 2003.
(36) Sadakane, M.; Steckhan, E. *Chem. Rev.* **1998**, *98*, 219 and references therein.

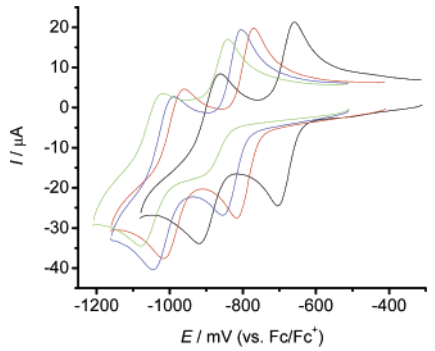

Figure 7. Experimental cyclic voltammograms of $[\alpha\text{-}PW_{11}O_{39}]^{7-}$ (1 mM) in buffered media at different pH values: 2.1 (black), 3.8 (red), 4.2 (blue), and 4.6 (green). Scan rate: 100 mV s^{-1}.

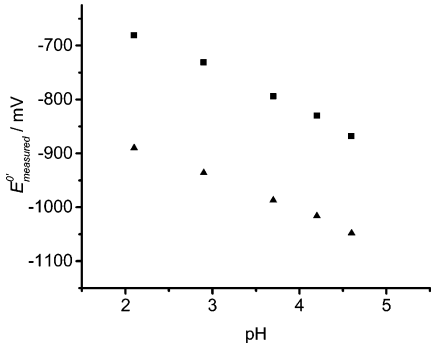

Figure 8. Plots of $E_{measured}^{\circ\prime}$ vs pH for both reduction processes of $[\alpha\text{-}PW_{11}O_{39}]^{7-}$ (1 mM) in the pH range studied. (■) Process **I**, (▲) process **II**.

acetonitrile (18.9). However, in the present case, it is the coupling of acid−base chemistry to the $[SiW_{11}O_{39}]^{8-/9-}$ process that produces a very large contribution to the reversible potential in water that is not a factor in dry aprotic solvent like CH_3CN.

Cyclic and Rotating Disk Electrode Voltammograms for Reduction of $[\alpha\text{-}PW_{11}O_{39}]^{7-}$ in Buffered Aqueous Media. Cyclic and rotating disk voltammograms of $[\alpha\text{-}PW_{11}O_{39}]^{7-}$ in buffered aqueous media in the pH range of 2.1−6.1 have similar characteristics to those found with $[\alpha\text{-}SiW_{11}O_{39}]^{8-}$ in the pH range of 2.1−6.8. Thus, the $E^{\circ\prime}$ values of the two $2e^-$ reduction processes of $[PW_{11}O_{39}]^{7-}$ (Table 6) are about 20 mV more positive than those of the reduction of $[SiW_{11}O_{39}]^{8-}$ at the same pH value (Table 4) where overall $2e^-$ processes were detected. This is as expected since the anionic charge of $[PW_{11}O_{39}]^{7-}$ is lower, which results in easier reduction.[3] A simple two $2e^-$ reduction mechanism ($A + 2e^- \rightleftharpoons B$, $B + 2e^- \rightleftharpoons C$) and the $E^{\circ\prime}$ values listed in Table 6 were used to simulate the RDE voltammograms at pH 2.1, which leads to a diffusion coefficient value of 3.0 ($\pm$0.1) $\times$ 10^{-6} cm^2 s^{-1}.

(37) Izutsu, K. *Electrochemistry in Nonaqueous Solutions*; Wiley: New York, 2002.

The $E^{\circ\prime}$ values of the two $2e^-$ reduction processes of $[PW_{11}O_{39}]^{7-}$ shifted to more negative potential as the pH increased. However, in this case, at pH 4.6, the peak current for the first $[PW_{11}O_{39}]^{7-}$ reduction wave decreased to about half, which is similar to the reduction behavior of $[SiW_{11}O_{39}]^{7-}$ at pH 6.1, which indicates that the pK_a value for $[PW_{11}O_{39}]^{7-}$ is less than that for $[SiW_{11}O_{39}]$.$^{8-}$ A plot of $E^{\circ\prime}$ vs pH for both reduction processes also show similar slopes (Figure 8), which implies that the difference in the number of protons in the oxidized and reduced forms ($m = 2.6$ for process **I** and $m = 2.4$ for process **II**) also are similar to those found when $[SiW_{11}O_{39}]^{8-}$ is reduced. Consequently, the same mechanism was proposed for reduction of $[PW_{11}O_{39}]^{7-}$ in aqueous media. However, since even the pK_a values for protonation of $[PW_{11}O_{39}]^{7-}$ are not available in the literature, the simulation was not attempted, as there were too many adjustable parameters.

Conclusions

The lacunary anions $[\alpha\text{-}SiW_{11}O_{39}]^{8-}$ and $[\alpha\text{-}PW_{11}O_{39}]^{7-}$ undergo only a simple $1e^-$ reduction in aprotic CH_3CN solution at very negative potentials just prior to the solvent limit. Addition of 0.3 equiv of acid to CH_3CN gives rise to a new reduction process at less negative potential which is attributed to the formation and reduction of the protonated species $[SiW_{11}O_{38}(OH)]^{7-}$. Analogous behavior is observed, but at less negative potentials for reduction of $[PW_{11}O_{39}]^{7-}$. Excellent agreement was obtained between voltammograms derived from simulations based on a double-square scheme and experimental ones found in the presence of acid. In contrast, proton reactions coupled to charge transfer contributes significantly to the voltammetry of these lacunary anions in buffered aqueous media over the pH range of about 2−6. A multi-square-scheme mechanism allows the essential thermodynamic and kinetic features of this system to be captured and also provides a detailed description of the various steps believed to be present, as well as their relative significance. Apparently, the very high overall negative charges associated with $[SiW_{11}O_{39}]^{8-}$ and $[PW_{11}O_{39}]^{7-}$ and their reduced forms makes these species so basic that they are able to remove protons from water. The presence of the acid−base chemistry coupled to the electron-transfer shifts reversible potentials to values a volt less negative than the E_F^0 value for the $[SiW_{11}O_{39}]^{8-/9-}$ and $[PW_{11}O_{39}]^{7-/8-}$ processes found in dry aprotic CH_3CN media.

Supporting Information Available: Key parameters used to simulate cyclic voltammograms presented in Figure 6b and c (Table S1). This material is available free of charge via the Internet at http://pubs.acs.org.

IC061081O